Ligand Based HQSAR Analysis of CRTh2 Antagonists

Sathya Babu and Thirumurthy Madhavan[†]

Abstract

CRTh2 receptor is an important mediator of the inflammatory effects and act as beneficial target for the treatment of asthma, COPD, allergic rhinitis and atopic dermatitis. In the present work, Hologram QSAR studies were conducted on a series of 50 training set CRTh2 antagonists (2-(2-(benzylthio)-1H-benzo[d]imidazol-1-yl acetic acids). The best HQSAR model was obtained using atoms, bonds, connections and donor/acceptor as fragment distinction parameter using hologram length 257 and 6 components with fragment size of minimum 7 and maximum 10. Significant cross-validated correlation coefficient (q^2=0.786) and non cross-validated correlation coefficients (r^2=0. 954) were obtained. The model was then used to evaluate the 15 external test compounds which are not included in the training set and the predicted values were in good agreement with the experimental results (r^2_{pred}=0.739). Contribution map show that presence of C ring and its substituents makes big contributions for activities. The HQSAR model and analysis from the contribution map could be useful for further design of novel structurally related CRTh2 antagonists.

Keywords: CRTh2, HQSAR

1. Introduction

Prostaglandin D2 (PGD2), a major metabolite of arachidonic acid is produced in high quantities by mast cells, particularly during IgE-dependent allergic responses[1-5]. PGD2 exhibit its biological responses by activating two seven transmembrane (7TM) G-protein coupled receptors (GPCRs), the classical DP1 receptor and chemoattractant receptor-homologous molecule expressed on T-helper 2 cells (CRTh2 also known as DP2) receptor[1-6]. CRTh2 is selectively expressed by Th2 cells, eosinophils and basophils and mediates chemotactic activation of these cells in response to prostaglandin D2 (PGD2)[1-7]. The interaction between immunologically activated mast cells and Th2 lymphocytes plays a key role in the pathogenesis of allergic disorders, and recent evidence suggests that CRTH2 plays a dominant role in mediating this interaction[2] and act as an important mediator in allergic reactions, including asthma, atopic dermatitis and allergic rhinitis[7-9]. There is also evidence that genetic alterations of

CRTh2 are linked to increased risk of allergy or asthma[10]. It is well established that antagonizing selectively the CRTh2 receptor could be useful in the treatment of asthma and other inflammatory disease[1,2,6,7].

Hologram Quantitative Structure Activity Relationship (HQSAR) is the novel 2D fragment-based QSAR method that employs specialized molecular fingerprints[11,12] and eliminates the need for 3D structure, molecular alignment and conformational search[13,14]. In HQSAR, each molecule in the training set is divided into several structural fragments, which are arranged to form a molecular hologram, assigned by a cyclic redundancy check (CRC) algorithm. In addition, HQSAR models interpret positive and negative contributions based on various atoms and structural units. Although HQSAR uses two dimensional information of a molecule, it also utilizes some three dimensional information such as chirality and molecular hybridization[15]. With HQSAR technique we can easily and rapidly generate QSAR models for both small and large data set with high predictive value compared to other QSAR models[11]. The limitation is that it could not make biological activity predictions accurately to molecules lacking fragments or structural units included in the training set which are used to set up the model. In the present study, HQSAR has been employed to study the activity of 65

Department of Bioinformatics, School of Bioengineering, SRM University, SRM Nagar, Kattankulathur, Chennai 603203, India.

[†]Corresponding author : thiru.murthyunom@gmail.com, thirumurthy.m@ktr.srmuniv.ac.in

CRTh2 antagonists. Many HQSAR models were generated with different combinations of parameters and based on statistical values of the model, the best model was selected and its contribution map was also analyzed. We also identified the important features of the compounds for improved activity. We hope that our models and analysis will be helpful for future design of novel and structurally related CRTh2 antagonists.

2. Materials and Methods

2.1. Data Set

The data set of CRTh2 antagonist reported by Pothier *et al*.[1] was used in this study. This includes a series of 65 compounds comprising of 2-(2-(benzylthio)-1H-

benzo[d]imidazol-1-yl acetic acids derivatives. The 65 compounds were segregated into a training set (50 compounds) and test set (15 compounds). The test set molecules were selected manually in order to cover all ranges of biological activity from the dataset. The given inhibitory concentration (IC_{50}) values were changed to minus logarithmic scale value (pIC_{50}) using the formula.

$$pIC_{50} = \log (IC_{50})$$

The structures and biological activities of all compounds including both training set and test set molecules is shown in Table 1. The HQSAR modeling analysis, calculations and visualization were performed using the molecular modeling package SYBYL-X 2.1.

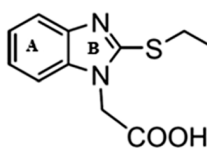**Table 1.** Structures and biological activities (pIC_{50}) of CRTh2 inhibitors
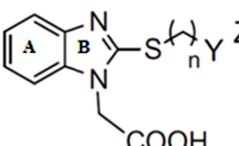
General template

a) Compound 1-17

Compound	n	Y	Z	pIC_{50} values
1	2	O	Phenyl	6.229
2	2	O	2-Naphthyl	5.602
3	2	O	1-Naphthyl	5.699
4	3	O	Phenyl	6.105
5	4	O	Phenyl	5.854
6	2	CH_2	Phenyl	6.323
7	1	CH_2	Phenyl	6.055
8	0	CH_2	Phenyl	6.411
9	3	NH	Phenyl	5.570
10	2	NH	Phenyl	5.114
11	4	CH_2	Methyl	5.867
12	3	CH_2	Methyl	5.907
13	2	CH_2	Methyl	5.625
14	1	CH_2	COOEt	4.943
15	2	CH_2	COOEt	5.356
16	3	CH_2	COOEt	5.627
17	4	CH_2	COOEt	5.996

Table 1. Continued

b) Compound 18-46
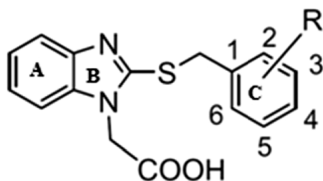
Compound	Substituent R at				pIC$_{50}$ values
	C(2)	C(3)	C(4)	C(5)	
18	H	H	Cl	H	6.796
19	H	Cl	H	H	6.731
20	Cl	H	H	H	6.432
21	H	H	OMe	H	6.678
22	H	OMe	H	H	7.143
23	OMe	H	H	H	5.959
24	H	H	Me	H	6.658
25	H	Me	H	H	6.979
26	Me	H	H	H	6.092
27	H	H	Br	H	6.658
28	H	Br	H	H	6.432
29	Br	H	H	H	6.237
30	H	H	CO$_2$Me	H	4.975
31	H	CO$_2$Me	H	H	6.347
32	CO$_2$Me	H	H	H	6.284
33	H	Cl	Cl	H	6.420
34	Cl	H	H	Cl	6.328
35	OMe	H	H	Me	5.921
36	OMe	H	H	Cl	6.131
37	OMe	H	H	OMe	5.796
38	OMe	H	H	CO$_2$Me	7.538
39	Br	CO$_2$Me	H	H	5.538
40	H	CO$_2$Me	Br	H	6.009
41	H	Br	H	CO$_2$Me	6.482
42	Br	H	H	CO$_2$Me	7.347
43	OMe	H	H	CO$_2$iPr	6.824
44	OMe	H	H	C(O)Me	8.097
45	H	H	H	C(O)Me	6.638
46	OMe	H	H	CH(OH)Me	5.657

Table 1. Continued

c) Compound 46-54
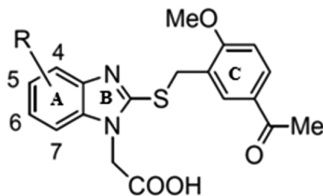
Compound	Substituent R at			pIC$_{50}$ values
	C(4)	C(5)	C(6)	
47	F	H	H	8.301
48	H	F	H	8.699
49	H	H	F	7.347
50	H	NO$_2$	H	8.699
51	H	CF$_3$	H	8.523
52	H	MeSO$_2$	H	7.387
53	H	Me(O)C	H	7.482
54	H	H(O)C	H	8.398

d) Compound 55-65
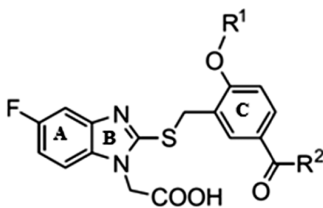
Compound	R^1	R^2	pIC$_{50}$ values
55	Et	Me	8.398
56	NPr	Me	8.301
57	NBu	Me	8.046
58	Me	Ph	8.770
59	Me	NHEt	7.796
60	Me	NHBu	7.796
61	Me	NHBn	7.229
62	Me	NEt$_2$	7.143
63	Me	NBnEt	6.305
64	Me	Morpholino	6.971
65	Me	Indolin-1-yl	8.523

The structures of the data set were sketched and minimized individually by using Powell's conjugate gradient method and Tripos force field.

2.2. HQSAR

HQSAR is a two dimensional computational technique that uses a fragmenting approaches that relates substructural components of compounds to their biological activity. In this method, each molecule is divided into a series of unique structural fragments that are counted in the bins of a fixed length array to form the molecular hologram[16]. The parameters such as hologram length, fragment size and fragment distinction affect the HQSAR model. The hologram length (HL)

determines the number of bins in the hologram into which the fragments are hashed. The optimal HQSAR model was derived from screening through the default HL values, which were set of prime numbers ranging from 53 to 401 to avoid fragment collisions. Fragment size controls the minimum and maximum length of the fragments to be included on the hologram fingerprint with the default as 4 and 7 respectively. Molecular fragment generation utilizes the following fragment distinctions: atoms (A), bonds (B), connections (C), chirality (Ch), hydrogen atoms (H) and donor/acceptor (DA). To evaluate the hologram generation, numerous models with the various combinations of the parameters were developed. The validity of the model depends on the statistical parameters such as cross-validated r^2 (q^2), non cross-validated r^2 by Leave-One-Out (LOO), r^2_{pred} and standard error. The predictive ability of HQSAR models was expressed using the following formula where SD is the sum of squared deviation between the biological activity of the test set and the mean activity of the training set molecules and the PRESS is the sum of squared deviations between predicted and observed activity value for every molecule ion the test set[17].

$$r^2_{pred} = (SD-PRESS)/SD$$

Once the structural information is encoded into the molecular hologram, HQSAR runs a PLS analysis to derive the HQSAR in which the molecular holograms generated were used as independent variables. The robustness of the model depends on the more challenging r^2_{pred} from the test set data.

3. Results and Discussion

3.1. HQSAR Analysis

HQSAR model generation was performed on 65 benzylthio imidazol acetic acid derivatives using three distinct parameters namely fragment size, hologram length and fragment distinction. 5 different combinations of training and test set molecules were used to develop HQSAR model and 15 HQSAR models using the different fragment distinction with the fragment size 4-7 were generated for each combination. Hence a total of 75 HQSAR models were generated in this study. The models generated using the combination of atoms, bonds, connections and donor/acceptor gave better results compared to others. The statistical results of the generated HQSAR models are shown in Table 2. The best model from each combination of training and test set were selected to further investigate the influence of length of fragment sizes (2-5, 3-6, 4-7, 5-8, 6-9, 7-10 and 8-11) and its results are summarized in Table 3. The

Table 2. HQSAR analysis for various fragment distinctions using default fragment size (4-7)

Model no	Fragment Distinction	q^2	r^2	SEE	N	HL
1	A/B	0.651	0.799	0.477	3	151
2	A/B/C	0.691	0.875	0.381	4	97
3	A/B/C/H	0.643	0.769	0.512	3	199
4	A/B/C/Ch	0.682	0.870	0.384	3	307
5	A/B/C/H/Ch	0.636	0.765	0.515	3	199
6	A/C/DA	0.642	0.928	0.295	6	307
7	A/B/C/H/DA	0.631	0.832	0.441	4	151
8	A/B/H	0.569	0.708	0.575	3	353
9	A/B/H/DA	0.599	0.795	0.487	4	307
10	**A/B/C/DA**	**0.708**	**0.892**	**0.353**	**4**	**257**
11	A/B/Ch/DA	0.626	0.735	0.542	2	307
12	A/B/H/Ch	0.569	0.709	0.574	3	307
13	A/B/DA	0.641	0.747	0.529	2	353
14	A/B/Ch	0.649	0.799	0.477	3	151
15	A/B/C/H/Ch/DA	0.641	0.821	0.455	4	199
16	A/B	0.620	0.786	0.496	3	151
17	A/B/C	0.630	0.849	0.416	3	307
18	A/B/C/H	0.555	0.723	0.564	3	199

Table 2. Continued

Model no	Fragment Distinction	q^2	r^2	SEE	N	HL
19	A/B/C/Ch	0.642	0.878	0.379	4	307
20	A/B/C/H/Ch	0.555	0.712	0.575	3	151
21	A/C/DA	0.575	0.848	0.422	4	257
22	A/B/C/H/DA	0.631	0.820	0.460	4	151
23	A/B/H	0.535	0.672	0.614	3	151
24	A/B/H/DA	0.569	0.771	0.518	4	151
25	**A/B/C/DA**	**0.668**	**0.920**	**0.314**	**6**	**307**
26	A/B/Ch/DA	0.635	0.874	0.389	5	151
27	A/B/H/Ch	0.534	0.664	0.621	3	151
28	A/B/DA	0.605	0.840	0.434	4	151
29	A/B/Ch	0.627	0.844	0.428	4	151
30	A/B/C/H/Ch/DA	0.584	0.810	0.472	4	151
31	A/B	0.671	0.813	0.442	3	151
32	A/B/C	0.761	0.924	0.288	5	97
33	A/B/C/H	0.656	0.798	0.459	3	199
34	A/B/C/Ch	0.736	0.905	0.319	4	97
35	A/B/C/H/Ch	0.682	0.917	0.305	6	199
36	A/C/DA	0.641	0.940	0.259	6	151
37	A/B/C/H/DA	0.725	0.892	0.344	5	151
38	A/B/H	0.612	0.751	0.510	3	307
39	A/B/H/DA	0.655	0.919	0.301	6	307
40	**A/B/C/DA**	**0.742**	**0.935**	**0.266**	**5**	**307**
41	A/B/Ch/DA	0.666	0.813	0.442	3	97
42	A/B/H/Ch	0.662	0.912	0.313	6	257
43	A/B/DA	0.671	0.818	0.436	3	97
44	A/B/Ch	0.672	0.810	0.446	3	151
45	A/B/C/H/Ch/DA	0.692	0.899	0.333	5	199
46	A/B	0.629	0.797	0.497	3	307
47	A/B/C	0.700	0.873	0.397	4	97
48	A/B/C/H	0.650	0.763	0.536	3	199
49	A/B/C/Ch	0.683	0.873	0.399	4	97
50	A/B/C/H/Ch	0.642	0.759	0.541	3	199
51	A/C/DA	0.633	0.907	0.347	6	97
52	A/B/C/H/DA	0.634	0.813	0.483	4	199
53	A/B/H	0.584	0.719	0.584	3	307
54	A/B/H/DA	0.612	0.788	0.513	4	307
55	**A/B/C/DA**	**0.689**	**0.873**	**0.398**	**4**	**307**
56	A/B/Ch/DA	0.628	0.738	0.559	2	353
57	A/B/H/Ch	0.586	0.715	0.589	3	307
58	A/B/DA	0.639	0.743	0.553	2	353
59	A/B/Ch	0.633	0.793	0.502	3	307
60	A/B/C/H/Ch/DA	0.652	0.819	0.475	4	199
61	A/B	0.628	0.778	0.505	3	151
62	A/B/C	0.609	0.795	0.480	3	97

Table 2. Continued

Model no	Fragment Distinction	q^2	r^2	SEE	N	HL
63	A/B/C/H	0.578	0.862	0.407	6	151
64	A/B/C/Ch	0.632	0.923	0.300	5	307
65	A/B/C/H/Ch	0.552	0.706	0.574	3	151
66	A/C/DA	0.572	0.791	0.485	3	353
67	A/B/C/H/DA	0.643	0.840	0.443	5	151
68	A/B/H	0.513	0.678	0.601	3	353
69	A/B/H/DA	0.564	0.753	0.532	4	151
70	**A/B/C/DA**	**0.682**	**0.908**	**0.328**	**5**	**307**
71	A/B/Ch/DA	0.637	0.741	0.533	2	307
72	A/B/H/Ch	0.509	0.683	0.596	3	353
73	A/B/DA	0.628	0.731	0.544	2	199
74	A/B/Ch	0.619	0.771	0.507	3	151
75	A/B/C/H/Ch/DA	0.598	0.837	0.437	5	151

Training set 1 (model 1-15): 2,7,11,14,19,25,29,34,39,42,47,53,57,60,63
Training set 2 (model 16-30): 2,8,14,16,20,24,28,33,38,43,48,53,57,61,64
Training set 3 (model 31-45): 2,6,11,14,19,25,30,34,37,42,48,53,56,60,64
Training set 4 (model 46-60): 2,8,13,16,20,24,28,33,40,42,47,53,57,61,63
Training set 5 (model 61-75): 1,5,12,17,21,24,28,35,39,44,48,52,56,60,64
The model chosen are highlighted in bold.
q2 – cross validated correlation coefficient; r2 –non cross validated correlation coefficient; SEE –standard error of estimate; N – number of statistical components; HL –hologram length; A–atoms; B –bonds; C –connections; H –hydrogen atoms; Ch – chirality; D/A donor and acceptor.

Table 3. Influence of various fragment size using the best fragment distinction combination (A/B/C/DA)

Model no	Fragment Size	q^2	r^2	SEE	N	HL
10	2-5	0.658	0.839	0.431	4	307
	3-6	0.686	0.863	0.397	4	307
	4-7	0.708	0.892	0.353	4	257
	5-8	0.705	0.936	0.275	5	257
	6-9	0.739	0.950	0.244	5	257
	7-10	**0.786**	**0.954**	**0.236**	**6**	**257**
	8-11	0.722	0.894	0.350	4	257
25	2-5	0.610	0.839	0.435	4	307
	3-6	0.621	0.850	0.420	4	307
	4-7	0.668	0.920	0.314	6	307
	5-8	0.644	0.917	0.316	5	257
	6-9	0.686	0.897	0.347	4	307
	7-10	**0.732**	**0.939**	**0.625**	**6**	**257**
	8-11	0.690	0.869	0.392	4	257
40	2-5	0.702	0.902	0.328	5	307
	3-6	0.727	0.902	0.328	5	307
	4-7	0.742	0.935	0.266	5	307
	5-8	0.761	0.960	0.212	6	257
	6-9	0.777	0.955	0.222	5	307
	7-10	**0.786**	**0.957**	**0.218**	**6**	**257**
	8-11	0.767	0.952	0.231	6	257

Table 3. Continued

Model no	Fragment Size	q^2	r^2	SEE	N	HL
55	2-5	0.664	0.832	0.457	4	307
	3-6	0.681	0.854	0.426	4	307
	4-7	0.689	0.873	0.398	4	307
	5-8	0.710	0.932	0.295	5	257
	6-9	0.729	0.946	0.262	5	257
	7-10	**0.771**	**0.954**	**0.244**	**6**	**257**
	8-11	0.702	0.885	0.382	4	257
60	2-5	0.635	0.848	0.423	5	307
	3-6	0.653	0.865	0.398	5	307
	4-7	0.682	0.908	0.328	5	307
	5-8	0.654	0.877	0.376	4	307
	6-9	0.707	0.853	0.406	3	307
	7-10	**0.709**	**0.884**	**0.364**	**4**	**257**
	8-11	0.678	0.826	0.442	3	257

The model chosen for further analysis are highlighted in bold.

Table 4. Statistical result of best HQSAR models using 7-10 fragment size and A/B/C/DA fragment distinction

No	Test Set Molecules	q^2	r^2	SEE	N	HL	r^2_{pred}
1	2,7,11,14,19,25,29,34,39,42,47,53,57,60,63	0.786	0.954	0.236	6	257	0.739
2	2,8,14,16,20,24,28,33,38,43,48,53,57,61,64	0.732	0.939	0.274	6	257	0.706
3	2,6,11,14,19,25,30,34,37,42,48,53,56,60,64	0.786	0.957	0.218	6	257	0.391
4	2,8,13,16,20,24,28,33,40,42,47,53,57,61,63	0.771	0.954	0.244	6	257	0.633
5	1,5,12,17,21,24,28,35,39,44,48,52,56,60,64	0.709	0.884	0.364	4	257	0.726

The final model is highlighted in bold.

Table 5. Experimental and predicted pIC50 values of training and test set compounds

Compound	Actual pIC_{50}	HQSAR	
		Predicted (pIC_{50})	Residual
1	6.229	6.097	0.132
2*	5.602	5.909	-0.307
3	5.699	5.825	-0.126
4	6.105	5.970	0.135
5	5.854	5.988	-0.134
6	6.323	6.041	0.282
7*	6.055	6.058	-0.003
8	6.411	6.434	-0.023
9	5.570	5.561	0.009
10	5.114	5.215	-0.101
11*	5.867	5.812	0.055
12	5.907	5.814	0.093
13	5.625	5.818	-0.193
14*	4.943	5.698	-0.755
15	5.356	5.838	-0.482
16	5.627	5.818	-0.191
17	5.996	5.766	0.230
18	6.796	6.548	0.248
19*	6.731	6.412	0.319

Table 5. Experimental and predicted pIC50 values of training and test set compounds

| Compound	Actual pIC_{50}	HQSAR	
		Predicted (pIC_{50})	Residual
20	6.432	6.487	-0.055
21	6.678	6.507	0.171
22	7.143	6.551	0.592
23	5.959	6.323	-0.364
24	6.658	6.420	0.238
25*	6.979	6.336	0.643
26	6.092	6.342	-0.251
27	6.658	6.357	0.301
28	6.432	6.362	0.070
29*	6.237	6.337	-0.100
30	4.975	5.293	-0.318
31	6.347	6.312	0.035
32	6.284	6.225	0.059
33	6.420	6.508	-0.088
34*	6.328	6.456	-0.128
35	5.921	6.008	-0.087
36	6.131	6.210	-0.079
37	5.796	5.819	-0.023
38	7.538	7.350	0.188
39*	5.538	6.225	-0.687
40	6.009	6.146	-0.137
41	6.482	6.163	0.319
42*	7.347	6.122	1.225
43	6.824	7.070	-0.246
44	8.097	7.972	0.125
45	6.638	7.017	-0.379
46	5.657	5.409	0.249
47*	8.301	8.299	0.002
48	8.699	8.374	0.325
49	7.347	7.516	-0.169
50	8.699	8.992	-0.293
51	8.523	8.542	-0.019
52	7.387	7.211	0.176
53*	7.482	8.541	-1.060
54	8.398	8.630	-0.232
55	8.398	8.344	0.054
56	8.301	8.542	-0.241
57*	8.046	8.580	-0.534
58	8.770	8.619	0.151
59	7.796	7.569	0.227
60*	7.796	7.515	0.281
61	7.229	7.375	-0.146
62	7.143	7.326	-0.183
63*	6.305	7.153	-0.848
64	6.971	6.947	0.024
65	8.523	8.402	0.121

*Test set compounds
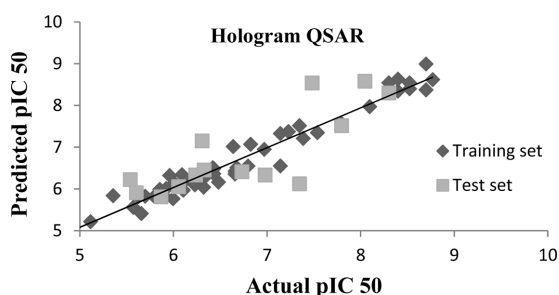
Fig. 1. Scatter plot diagram of predicted versus actual activity of training set and test set compounds by HQSAR analyses.

statistical parameters showed that there is significant improvement by changing the fragment size. Larger fragment size was favored for improving statistical results in the form of q^2 and r^2 value. We had chosen the best model with higher q^2 and lower SEE values as summarized in Table 3 for examining the predictive

ability of test set molecules. The statistical values of the best models with different training and test set compounds along with its r^2_{pred} are tabulated in Table 4. Based on better q^2 and r^2_{pred} values the final model was selected (q^2=0.786, r^2=0.954, SEE=0.236, r^2_{pred} =0.739) which was built using parameters A/B/C/DA as fragment distinction, fragment size set to min 7 and max 10 with hologram length 257 and 6 components. The detailed predicted versus actual activities along with the residual values for training and test set was depicted in Table 5 and plotted in Fig. 1. Low residual values obtained for developed HQSAR model indicates its reliability and can be used to predict the biological activity of novel compounds.

3.2. HQSAR Contribution Map Analysis

The HQSAR results gave direct evidence about the individual atomic contributions to the biological activity through the use of different color codes. The contribu-
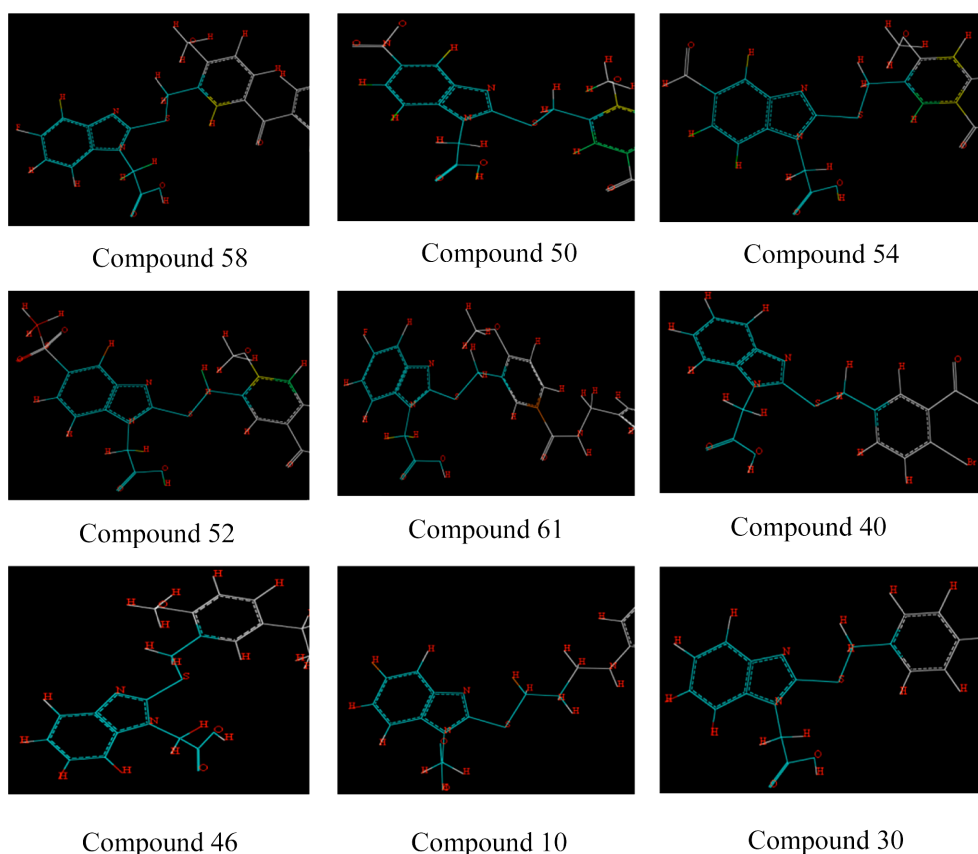

Compound 58   Compound 50   Compound 54

Compound 52   Compound 61   Compound 40

Compound 46   Compound 10   Compound 30

Fig. 2. HQSAR contribution map.

tions of the different fragments for the activity of the molecules are displayed in Fig. 2. The colors at the red end of the spectrum indicates the poor contributions (red, red orange and orange), while colors at the green end reflect favorable contributions (yellow, green blue and green). Atoms with intermediate contributions are colored in white.

In the contribution map we found that the scaffold of benzylthio imidazol derivatives are represented in white in all compounds which depicts the intermediate contribution of scaffold in the activity of all molecules. The generated HQSAR model for few compounds is shown in Figure 2 where the A and B ring are colored in cyan color which indicates the common substructure and it contributes to the inhibitory activity of the compound. In the highly active compounds (58, 50 and 54), the C ring is covered by green and yellow color and also the CH$_3$ groups attached to it is covered by green which confirms of the presence of C ring and its substituents are strongly responsible for the improved activity. For the compound 52, the presence of MeSO$_2$ attached to the A ring indicates that this may be the reason for its intermediate activity. The compounds from 1 to 18 does not have C ring and hence does not show either good or poor contribution. The compounds such as 46, 10 and 30 have lower activity then others and its contribution map shows that the presences of H at the A ring are alone highlighted in red and brown which normally depicts the poor contributions.

4. Conclusion

This study was conducted to rationalize the benzylthio imidazol acetic acid derivatives by HQSAR analysis. All the generated models showed good statistical results in terms of q^2 and r^2 values. The best model was selected based on high q^2 (0.786) and r$^2_{pred}$ (0.739) values. Contribution map show that presence of C ring and its substituents makes favorable contributions in the highly active compounds. This study is useful for the discovery of novel antagonists for CRTh2 receptor.

References

[1] J. Pothier, M. A. Riederer, O. Peter, X. Leroy, A. Valdenaire, C. Gnerre, and H. Fretz, "Novel 2-(2-(benzylthio)-1H-benzo[d]imidazol-1-yl)acetic acids: Discovery and hit-to-lead evolution of a selective CRTh2 receptor antagonist chemotype", Bioorg. Med. Chem. Lett., Vol. 22, pp. 4660-4664, 2012.

[2] R. Pettipher and M. Whittaker, "Update on the development of antagonists of chemoattractant receptor-homologous molecule expressed on Th2 Cells (CRTH2). From lead optimization to clinical proof-of-concept in asthma and allergic rhinitis", J. Med. Chem., Vol. 55, pp. 2915-2931, 2012.

[3] D. Bonafoux, A. Abibi, B. Bettencourt, A. Burchat, A. Ericsson, C. M. Harris, T. Kebede, M. Morytko, M. McPherson, G. Wallace, and X. Wu, "Thienopyrrole acetic acids as antagonists of the CRTH2 receptor", Bioorg. Med. Chem. Lett., Vol. 21, pp. 1861-1864, 2011.

[4] T. Ulven and E. Kostenis, "Novel CRTH2 antagonists: a review of patents from 2006 to 2009", Expert Opin. Ther. Pat., Vol. 20, pp. 1505-1530, 2010.

[5] A. N. Hata, T. P. Lybrand, and R. M. Breyer, "Identification of determinants of ligand binding affinity and selectivity in the prostaglandin D2 receptor CRTH2", J. Biol. Chem., Vol. 280, pp. 32442-32451, 2005.

[6] K. J. Abhishek, N. Manochac, V. Ravichandrana, V. K. Mouryab, and R. K. Agrawala, "Three-dimensional Qsar study of 2,4-disubstituted-phenoxy acetic acid derivatives as a Crth2 receptor antagonist: Using the K-nearest neighbor method", Dig. J. Nanomater. Bios., Vol. 3, pp. 147-158, 2008.

[7] T. N. Birkinshaw, S. J. Teague, C. Beech, R. V. Bonnert, S. Hill, A. Patel, S. Reakes, H. Sanganee, I. G. Dougall, T. T. Phillips, S. Salter, J. Schmidt, E. C. Arrowsmith, J. J. Carrillo, F. M. Bell, S. W. Paine, and R. Weaver "Discovery of potent CRTh2 (DP2) receptor antagonists", Bioorg. Med. Chem. Lett., Vol. 16, pp. 4287-4290, 2006.

[8] S. Crosignani, P. Page, M. Missotten, V. Colovray, C. Cleva, J.-F. Arrighi, J. Atherall, J. Macritchie, T. Martin, Y. Humbert, M. Gaudet, D. Pupowicz, M. Maio, P.-A. Pittet, L. Golzio, C. Giachetti, C. Rocha, G. Bernardinelli, Y. Filinchuk, A. Scheer, M. K. Schwarz, and A, Chollet, "Discovery of a new class of potent, selective, and orally bioavailable CRTH2 (DP2) receptor antagonists for the treatment of allergic inflammatory diseases", J. Med. Chem., Vol. 51, pp. 2227-2243, 2008.

[8] R. Pettipher, "The roles of the prostaglandin D2 receptors DP1 and CRTH2 in promoting allergic responses", Brit. J. Pharmacol., Vol. 153, pp. 191-199, 2008.

[10] N. Kaila, B. Follows, L. Leung, J. Thomason, A. Huang, A. Moretto, K. Janz, M. Lowe, T. S. Mansour, C. Hubeau, K. Page, P. Morgan, S. Fish, X. Xu, C. Williams, and E. Saiah, "Discovery of isoquinolinone indole acetic acids as antagonists of chemoattractant acceptor homologous molecule expressed on Th2 Cells (CRTH2) for the treatment of allergic inflammatory diseases", J. Med. Chem., Vol. 57, pp. 1299-1322, 2014.

[11] Tripos Sybyl, HQSAR manual.

[12] C. L. Waller, "A comparative QSAR study using CoMFA, HQSAR, and FRED/SKEYS paradigms for estrogen receptor binding affinities of structurally diverse compounds", J. Chem. Inf. model., Vol. 44, pp. 758-765, 2004.

[13] W. Tong, D. R. Lowis, R. Perkins, Y. Chen, W. J. Welsh, D. W. Goddette, T. W. Heritage, and D. M. Sheehan, "Evaluation of quantitative structure-activity relationship methods for large-scale prediction of chemicals binding to the estrogen receptor",

J. Chem. Inf. model., Vol. 38, pp. 669-677, 1998.

[14] T. W. Heritage and D. R. Lowis, "Molecular hologram QSAR. In rational drug design", M. R., Eds, ACS Symposium Series 719, American Chemical Society, pp 212, 2000.

[15] M. A. Avery, M. A. Gaston, C. R. Rodrigues, E. J. Barreiro, F. E. Cohen, Y. A. Sabnis, and J. R. Woolfrey, "Structureactivity relationships of the antimalarial agent artemisinin. 6. The development of predictive in vitro potency models using CoMFA and HQSAR methodologies", J. Med. Chem., Vol. 45, pp. 292-303, 2002.

[16] D. A. Winker and F. R. Burden, "Holographic QSAR of benzodiazepines", Quantitative Structure-Activity Relationships, Vol. 17, pp. 224-231, 1998.

[17] R. D. Cramer, D. E. Patterson, and J. D. Bunce, "Comparative molecular field analysis (CoMFA), 1. Effect of shape on binding of steroids to carrier proteins", J. Am. Chem. Soc., Vol. 110, pp. 5959-5967, 1988.